online data

SLC41A2 encodes a plasma-membrane Mg^{2+} transporter

Jaya SAHNI*, Bruce NELSON† and Andrew M. SCHARENBERG*[1]

*Department of Pediatrics, University of Washington, and Children's Hospital and Regional Medical Center, Suite 300, 307 Westlake Avenue North, Seattle, WA 98195, U.S.A., and †Department of Geology, Laboratory of Geochemistry, University of Washington, Seattle, WA 98195, U.S.A.

The TRPM7 (transient receptor potential melastatin 7) ion channel has been implicated in the uptake of Mg^{2+} into vertebrate cells, as elimination of TRPM7 expression through gene targeting in DT40 B-lymphocytes renders them unable to grow in the absence of supplemental Mg^{2+}. However, a residual capacity of TRPM7-deficient cells to accumulate Mg^{2+} and proliferate when provided with supplemental Mg^{2+} suggests the existence of Mg^{2+} uptake mechanism(s) other than TRPM7. Evaluation of the expression of several members of the SLC41 (solute carrier family 41) family, which exhibit homology with the MgtE class of prokaryotic putative bivalent-cation transporters, demonstrated that one, SLC41A2 (solute carrier family 41 member 2), is expressed in both wild-type and TRPM7-deficient DT40 cells. Characterization of heterologously expressed SLC41A2 protein indicated that it is a plasma-membrane protein with an N-terminus-outside/C-terminus-inside 11-TM (transmembrane)-span topology, consistent with its functioning as a trans-plasma-membrane transporter. In contrast with a previous report of ion-channel activity associated with SLC41A2 expression in oocytes, investigation of whole cell currents in SLC41A2-expressing DT40 cells revealed no novel currents of any type associated with SLC41A2 expression. However, expression of SLC41A2 in TRPM7-deficient cells under the control of a doxycycline-inducible promoter was able to conditionally enhance their net uptake of $^{26}Mg^{2+}$ and conditionally and dose-dependently provide them with the capacity to grow in the absence of supplemental Mg^{2+}, observations strongly supporting a model whereby SLC41A2 directly mediates trans-plasma-membrane Mg^{2+} transport. Overall, our results suggest that SLC41A2 functions as a plasma-membrane Mg^{2+} transporter in vertebrate cells.

Key words: DT40 B-lymphocytes, Mg^{2+} transporter, solute carrier family 41 member 2 (SLC41A2), transient receptor potential melastatin 7 (TRPM7).

INTRODUCTION

Mg^{2+} plays a central role in myriad metabolic and biochemical processes essential for life, most notably as a cofactor for ATP. Accordingly, vertebrate organisms expend substantial energy to maintain their overall Mg^{2+} homoeostasis by recovering Mg^{2+} from urine, and proliferating cells expend substantial energy to maintain cellular Mg^{2+} homoeostasis by taking up Mg^{2+} from extracellular fluids. As both organism and cellular Mg^{2+} homoeostasis are dependent on regulated TM (transmembrane) Mg^{2+} transport, a molecular-level understanding of Mg^{2+} transport is of fundamental significance to understanding vertebrate metabolism.

Over the past 2 years, three classes of proteins have been suggested to function as vertebrate Mg^{2+} transporters: (1) TRPM6 (transient receptor potential melastatin 6) and TRPM7, novel dual-function ion channel/protein kinases, have been implicated in trans-plasma-membrane Mg^{2+} uptake via an ion-channel mechanism by genetic studies of human patients with TRPM6 mutations and biochemical and electrophysiological analyses of TRPM7-deficient and TRPM7-overexpressing cells [1–3]; (2) SLC41 (solute carrier family 41) proteins, which are distant homologues of prokaryotic MgtE transporters, have been implicated in Mg^{2+} transport via an ion-channel mechanism through electrophysiological studies in SLC41-RNA-injected *Xenopus* oocytes [4–6]; and (3) MagT1, a protein which is homologous with the yeast OST (oligosaccharyl transferase) complex protein OST3/OST6, has also been implicated in Mg^{2+} transport via an ion-channel mechanism through electrophysiological studies of MagT1-RNA-injected *Xenopus* oocytes [7]. However, although supplemental Mg^{2+} has been shown to rescue the respective TRPM6 and TRPM7 deficiency phenotypes, supporting direct or indirect roles for these proteins in a pathway capable of substantial trans-plasma membrane Mg^{2+} transport, no data have been reported regarding whether, and to what extent, SLC41 proteins or MagT1 are involved in intracellular inter-compartmental Mg^{2+} transport or trans-plasma-membrane Mg^{2+} uptake from extracellular fluids in vertebrate cells.

In the present study we have further characterized the Mg^{2+}-transport phenotype of TRPM7-deficient DT40 cells and explored their use as a tool for identifying novel vertebrate Mg^{2+} uptake mechanisms. We show that TRPM7-deficient DT40 cells express a native SLC41 protein, SLC41A2, and demonstrate that heterologously expressed SLC41A2 is a cell-surface protein with a likely 11-TM-span N-terminus-out/C-terminus-in topology. In addition, we have analysed the influence of heterologously expressed SLC41A2 proteins on Mg^{2+} homoeostasis in the context of TRPM7-deficient DT40 cells. Overall, our results indicate that SLC41A2 proteins act as physiologically significant trans-plasma-membrane Mg^{2+} transporters in vertebrate cells.

EXPERIMENTAL

Cell lines

DT40 cells were maintained in RPMI 1640 medium supplemented with 10 % (v/v) FBS (fetal bovine serum), 1 % chicken serum

Abbreviations used: FBS, fetal-bovine serum; HEK-293, human embryonic kidney epithelial cell line 293; ICP-MS, inductively coupled plasma MS; -KO, -knockout; MagNuM, Mg^{2+}-nucleotide-regulated metal-ion current; MIC, Mg^{2+}-inhibited cation current; OST, oligosaccharyltransferase; PE, phycoerythrin; SLC41A2, solute carrier family 41 member 2; RT-, reverse transcription; TM, transmembrane; TRPM7, transient receptor potential melastatin 7; WT, wild-type.

[1] To whom correspondence should be addressed (email andrewms@u.washington.edu).

10 units/ml penicillin/streptomycin and 2 mM glutamine. HEK-293 (human embryonic kidney epithelial cell line 293) cells were maintained in Dulbecco's modified Eagle's medium with 10 % FBS.

RT-PCR analysis of SLC41A2 expression in WT (wild-type), TRPM7-KO (TRPM7-knockout) DT40 B-cells and immune lineage (B- and T-cells) cells

Gradient reverse-transcription (RT)-PCR analysis was performed on cDNA synthesized from total RNA extracted using a TRIzol/Qiagen RNeasy Mini Kit. Genomic DNA contamination was removed by treatment with RNase-free DNase. For analysing DT40 SLC41A2 expression the oligonucleotides were used to produce a 979-bp product: forward, 5′-GTTAAATCTGACCAG-CACGTGGAG-3′; and reverse, 5′-GGATCAGATGTTGTGTC-CAGAATAAGG-3′. PCR was performed using standard techniques, with an initial cycle of 94 °C for 2 min, followed by 30 cycles of 94 °C for 40 s, gradient 50–74 °C for 30 s, 72 °C for 3 min and a final extension at 72 °C for 5 min. Detection of human SLC41A2 transcripts by RT-PCR was also carried out on cDNA synthesized from RNA of Jurkat (human T cell leukaemia), Raji, Ramos (human Burkitt's lymphoma cell lines), Nalm-6 (human B cell precursor leukaemia), OCI-Ly3 and OCI-Ly10 (B-cell-like DLBCL cell lines) cells. The internal primer pair used was as follows: forward, 5′-CTTGCCATATTGGCTTGGAT-3′; and reverse, 5′-CAACCTTTGGGTTCATCAGG-3′. The PCR protocol was as follows: 94 °C for 2 min, followed by 35 cycles of 94 °C for 30 s, 59 °C for 30 s, 72 °C for 1 min 15 s and a final extension at 72 °C for 5 min. The amplicon size was 374 bp and was analysed on a 1.5 %-(w/v)-agarose gel.

Cloning, expression and analysis of human SLC41A2

RT-PCR was used to isolate human SLC41A2 cDNA from the Jurkat T-cell line. The primers used were as follows: forward, 5′-ATGGAGTATCACAGTTTCTCAGAGCAG-3′; and reverse, 5′-GTCTCCAACATCTCCATCTCGATC-3′. Subsequently the cDNA containing the open reading frame of SLC41A2 was PCR-amplified using the following primers: forward, 5′-GACGCGGC-CGCTGGAGTATCACAGTTTCTCAGAGCA-3′, and reverse, 5′-CGGTCTAGATTAGTCTCCAACATCTCCATCTCG-3′. The PCR cycle used was: 94 °C for 2 min, followed by 34 cycles of 94 °C for 30 s, 62 °C for 40 s, 72 °C for 3 min and a final extension at 72 °C for 5 min. The coding sequence was fused at the 5′-end to a Kozak sequence, a sequence encoding the FLAG epitope tag and an additional in-frame NotI site, GCGGCCGC. At the 3′-end an XbaI site was added downstream of the stop codon. The PCR product encodes a modified protein which starts with the amino acid sequence MGDYKDDDDKRPL followed by the human SLC41A2 (as per the amino acid sequence in GenBank®, accession number NP_115524) coding sequence starting from the second amino acid and was cloned into the pcDNA4/TO vector (Invitrogen), which provides a tetracycline-controlled expression from a human cytomegalovirus immediate early promoter. The FLAG–SLC41A2/pcDNA4/TO construct was transfected by electroporation into HEK-293 and TRPM7-KO DT40 cells expressing the tet repressor protein (via previous stable transfection with pCDNA6/TR), and clones were selected with zeocin (0.4 mg/ml; Invitrogen). The resistant clones were analysed for tetracycline-induced FLAG–SLC41A2 expression by immunoprecipitation and Western blotting. Comparison of growth rates between the DT40-WT, TRPM7-KO cells, TRPM7-KO complementing FLAG–SLC41A2 and FLAG–SLC41A2-HA expressing cells was performed by seeding the cells at an initial cell density of 2×10^5/ml, following which they were counted at 24, 48 and 72 respectively. At certain time points in the experiment described in Figure 5 (below), the cells were split back to the seeding cell density, so as to make sure that the medium was not a limiting factor and that the cells did not enter the stationary growth phase. Following those time points, cell numbers shown in the graph were calculated by multiplying the pre-split cell number with the number of times they multiplied by the next cell count.

Electrophoresis, immunoprecipitations and Western blotting

SDS/PAGE was carried out according to the Laemmli method using 10 %-(w/v)-acrylamide gels. Whole-cell lysates were prepared by lysing the cells in ice-cold lysis buffer (150 mM NaCl, 50 mM Tris, pH 7.5, and 1 % Triton X-100, supplemented with protease inhibitors). The lysate was rotated for 45 min at 4 °C, followed by centrifugation at 20 000 ***g*** for 10 min. Protein concentration was determined by the Bradford assay. Anti-FLAG (anti-FLAG M2 affinity gel; Sigma), anti-HA (anti-haemagglutinin; HA-Tag Mouse mAb; Cell Signaling) or anti-SLC41A2 (polyclonal antibody raised against an N-terminal peptide of the human SLC41A2; Zymed) immunoprecipitations were performed on pre-cleared cell lysates of DT40 and HEK-293 cells at 4 °C by addition of Protein A–Sepharose beads (for HA-tag and SLC41A2 immunoprecipitations). Subsequently, the beads were washed three times with lysis buffer, resuspended in sample loading buffer and boiled for 1–5 min. Aliquots of the supernatant were separated by SDS/10 %-PAGE. Proteins were transferred to PVDF membrane (Millipore) and were blocked in 5 % blocking buffer overnight {5 % (w/v) non-fat dried milk in TBS [Tris-buffered saline (140 mM NaCl and 20 mM Tris/HCl, pH 7.5)]/0.1 % Tween-20}. Bound antibody was detected by the Amersham ECL® (enhanced chemiluminescence) detection system.

$^{26}Mg^{2+}$ uptake assay

The stable magnesium isotope $^{26}Mg^{2+}$ (85–90 atom % ^{26}Mg) was obtained as ^{26}MgO from Isotec, Miamisburg, OH, U.S.A. Cells were washed and incubated in media containing 0.4 mM $^{26}Mg^{2+}$ (normal Mg^{2+} media concentration) for different time periods at 37 °C. Following incubation the cells were lysed with 0.1 M HCl and submitted for ICP-MS (inductively coupled plasma MS) [8,9]. Changes in the $^{26}Mg^{2+}/^{24}Mg^{2+}$ ratio over time provided a measure of the rate at which each cell type was able to take up and accumulate Mg^{2+}.

Membrane topology analysis by flow cytometry

For FACS analysis, TRPM7-KO DT40 B-cells (1×10^6) expressing either FLAG-SLC41A2 or FLAG-SLC41A2-HA were stained with the specific primary antibody (α-FLAG/α-HA) or the isotype control, mouse IgG1-UNLB, (Southern Biotech) at 4 °C for 30 min. Anti-FLAG M2 antibody was obtained from Sigma (catalogue no. F3165) and anti-HA antibody from Cell Signaling (catalogue no. 2367). For detection of intracellular epitopes, cells were fixed and permeabilized with Fixation/Permeabilization solution (BD Cytofix/Cytoperm™ Fixation/Permeabilization kit; catalogue no. 554714) at 4 °C for 20 min, prior to incubation with the antibody. Live cells were washed twice with PBS + 1 % BSA and fixed cells were washed with the BD Perm/Wash™ buffer (1×). Further, cells were incubated with either anti-mouse–FITC or PE (phycoerythrin) (FITC for FLAG and PE for HA tag) secondary antibodies at 4 °C for 30 min and washed twice. Cells were resuspended in PBS + 1 % BSA and analysed on BD FACSCalibur™ flow cytometer.

Analysis of regulated gene expression of *SLC41A2*

DT40 TRPM7-KO cells expressing FLAG–SLC41A2 under control of a tet-inducible promoter were grown in RPMI 1640 containing tetracycline-free 10 % (v/v) FBS (BD Biosciences). To compare their growth rates, under various doses of doxycycline, cells were cultured in four different concentrations of doxycycline, namely 1 μg/ml, 1 ng/ml, 500 pg/ml and 200 pg/ml. Cells were seeded at an initial cell density of 1×10^5/ml, following which the cells were counted at 24, 48 and 72 h. At the 48 h time point, cells were split back to the seeding cell density in order to make sure that the medium was not a limiting factor and that the cells did not enter the stationary growth phase. For expression analysis, immunoblotting was carried out on the cell lysates with the α-FLAG monoclonal antibody. Regulated FLAG–SLC41A2 expression was also analysed by flow cytometry. Briefly, 1×10^6 TRPM7-KO DT40 cells expressing FLAG–SLC41A2 under doxycycline doses of 1 μg/ml, 1 ng/ml, 500 pg/ml and 200 pg/ml were stained with α-FLAG antibody at 4 °C for 30 min. Following two washes with PBS + 1 % BSA, cells were incubated in the secondary antibody (anti-mouse–FITC) at 4 °C for 30 min and washed twice. Cells were further resuspended in PBS + 1 % BSA and analysed using the FACSCalibur instrument.

Electrophysiology

WT and TRPM7-KO DT40 B-cells were previously described [2]. TRPM7-KO clone cSLC (stably transfected with pcDNA4-TO/FLAG-human SLC41A2 construct driving tetracycline-inducible SLC41A2 expression) were constructed as described above. Cells were grown in RPMI supplemented with 10 % FBS, blasticidin (50 μg/ml) and zeocin (0.4 mg/ml). Expression of *SLC41A2* was induced by adding 1 μg/ml doxycycline to the culture medium.

Whole-cell patch-clamp experiments were performed at 21–25 °C approx. 2–4 h after cells were plated on glass coverslips and kept in a modified Ringer's solution of the following composition (in mM): NaCl, 145; KCl, 2.8; CsCl, 10; $CaCl_2$, 1; $MgCl_2$, 2; glucose, 10: Hepes/NaOH, 10; pH 7.2. For experiments performed with strong chelation of Mg^{2+} and Ca^{2+}, an EDTA Ringer's solution (NaCl, 145; KCl, 2.8; CsCl, 10; $CaCl_2$, 1; $MgCl_2$, 2; glucose, 10; Hepes/NaOH, 10; EDTA, 5; pH 7.2) was created. Nominal-zero intracellular pipette-filling solutions contained (in mM): caesium glutamate, 145; NaCl, 8; caesium EGTA, 10; Hepes/CsOH, 10; pH 7.2. Intracellular pipette-filling solutions with strong chelation of Mg^{2+} and Ca^{2+} contained (in mM): caesium glutamate, 145; NaCl, 8; caesium EGTA, 5; sodium EDTA, 5; Hepes/CsOH, 10; pH 7.2. High-resolution current recordings were acquired by a computer-based patch-clamp amplifier system (EPC-9; HEKA, Lambrecht, Germany). Immediately following establishment of the whole-cell configuration, voltage ramps of 50 ms duration spanning the voltage range of -100 to $+100$ mV were delivered from a holding potential of 0 mV at a rate of 0.5 Hz over a period of 300–400 s. All voltages were corrected for a liquid junction potential of 10 mV between external and internal solutions when internal solutions contained glutamate. Currents were filtered at 2.3 kHz and digitized at 100 μs intervals. Capacitive currents and series resistance were determined and corrected before each voltage ramp using the automatic capacitance compensation of the EPC-9. The low-resolution temporal development of currents at a given potential was extracted from individual ramp current records by measuring the current amplitudes at voltages of -80 mV or $+80$ mV. Outward currents are reported for presentation purposes because of their larger magnitude relative to background and unequivocal correlation with TRPM7 activation.

RESULTS

Analysis of SLC41 family protein expression in DT40 cells

TRPM7-deficient DT40 cells exhibit a defect in growth which can be complemented by provision of increased concentrations of extracellular Mg^{2+} [2]. This phenotype implicates TRPM7 as a key mediator or regulator of Mg^{2+} uptake and, in addition, suggests the existence of at least one alternative trans-plasma-membrane Mg^{2+}-transport mechanism. In a search for potential new types of Mg^{2+} transporters which might account for the residual Mg^{2+} transport capacity of TRPM7-deficient DT40 cells, we identified a group of proteins that have homology with the prokaryotic MgtE family of multispan membrane proteins, several members of which have been shown to mediate uptake of Mg^{2+} and other bivalent cations in bacterial systems [10–13]. These proteins have been previously designated as the SLC41 family [6]. As these proteins appeared to be viable candidates for mediating the residual Mg^{2+}-transport capacity of DT40 cells, we utilized database searching to identify two chicken predicted proteins (GenBank® accession numbers CAG32667/XP_425486 and XP_414373) with close homology with three proteins which make up the human SLC41 family [6]. On the basis of sequence comparisons, the protein represented in CAG32667/XP_425486 (XP_425486 has now been replaced by NP_001026654) is considered to be the orthologue of human SLC41A2, whereas XP_414373 appears to be the human SLC41A1 orthologue.

Using portions of expressed-sequence-tag sequences corresponding to these proteins, we performed gradient RT-PCR analyses of both WT DT40 cells and TRPM7-KO cells to define SLC41 family expression in the DT40 cells. These experiments indicated the presence of chicken SLC41A2 transcripts in both WT and TRPM7-KO cell lines (Figure 1A). We were not able to amplify cDNA transcripts for either the chicken SLC41A1 or any of several SLC41A3 variants, despite utilizing primers and conditions able to amplify genomic sequences (results not shown). These results indicate that DT40 cells dominantly express a single SLC41 family transcript encoding a protein which is the orthologue of human SLC41A2. SLC41A2 transcripts were also detectable in Jurkat, Raji, Ramos, Nalm-6, OCI-Ly3 and OCI-Ly10 cells, suggesting that SLC41A2 is ubiquitously expressed in immune lineage cells (Figure 1B). We also compared SLC41A2 expression in WT and TRPM7-deficient DT40 cells using quantitative PCR, and found that SLC41A2 expression was up-regulated in the TRPM7-deficient cells (results not shown). The up-regulation of *SLC41A2* expression in response to loss of the Mg^{2+}-uptake mediated/regulated by TRPM7 further supported the hypothesis that SLC41A2 proteins mediate a portion of the residual Mg^{2+} transport in TRPM7-deficient DT40 cells.

Cloning, expression and characterization of heterologously expressed SLC41A2 proteins

As a first step towards analysing the function of SLC41A2 proteins, we cloned and sequenced full-length chicken and human SLC41A2 cDNAs (from DT40 cells and Jurkat T-cells respectively) and found them to be highly homologous, exhibiting over 90 % identity throughout their sequences (see Supplementary Figure 1 at http://www.BiochemJ.org/bj/401/bj4010505add.htm). The SLC41A2 sequence identified in DT40 cells is nearly identical with a chicken SLC41A2 protein represented by NP_001026654, with the exception of a single amino acid difference at position 24 (valine substituted for glycine) in the DT40 sequence (this difference probably reflects a sequence difference between the DT40 cell line and the chicken species from which the GenBank sequence was derived). The level of identity

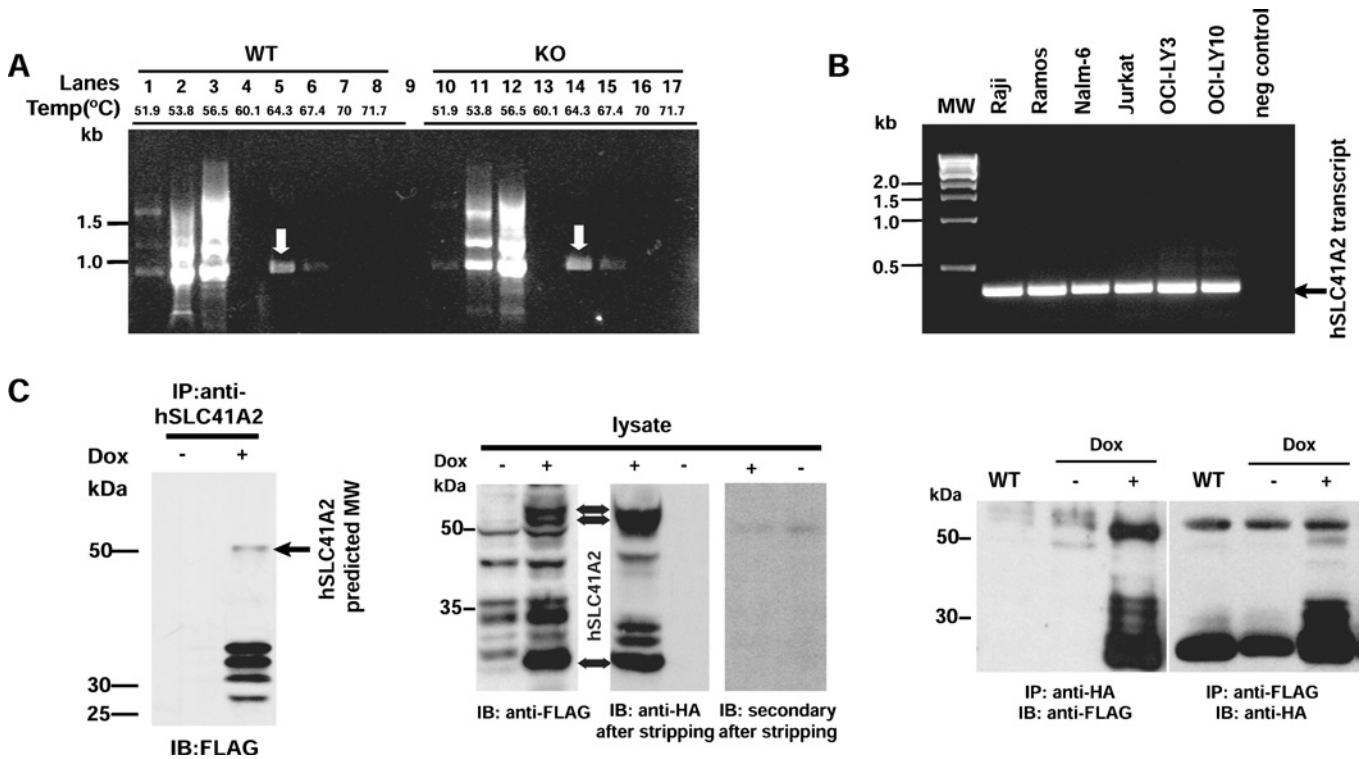

Figure 1 SLC41 expression and functional characterization

(**A**) Analysis of expression of chicken SLC41A2 (homologous with human SLC41A2) by gradient RT-PCR (51.9–71.7 °C) in WT DT40 and TRPM7-KO clones grown in presence of 15 mM supplemental Mg^{2+}. A 979 bp fragment was observed in both the cell lines at 64.3 °C (as indicated by the white arrows) and was confirmed by sequence analysis to represent chicken SLC41A2 transcript (lanes 1–8, WT DT40 cDNA; lanes 10–17, TRPM7-KO cDNA). Lanes 4 and 13 were negative controls and lane 9 was empty. (**B**) RT-PCR analysis of SLC41A2 transcript expression in cells of immune lineage (B- and T-cells). Expression analysis included the Jurkat T cell line and Raji, Ramos, Nalm-6, OCI-LY3 and OCI-LY10 B cell lines. A 374 bp band was observed in all the cell lines with a human SLC41A2 internal primer pair. (**C**) Heterologous expression of SLC41A2. Left panel: HEK-293 cells were transfected with a doxycycline (Dox)-regulated FLAG-SLC41A2 cDNA, and expression was analysed by SDS/PAGE, immunoprecipitation (IP) with anti-SLC41A2 N-terminal antibody and immunoblotting (IB) with anti-FLAG. Middle panel: expression of doxycycline-regulated FLAG-SLC41A2-HA was analysed by SDS/PAGE and immunoblotting with anti-FLAG antibody to demonstrate the presence of the N-terminal tag. The membrane was then stripped, initially reblotted with secondary antibody alone to demonstrate the removal of anti-FLAG, and subsequently reblotted with anti-HA to demonstrate the presence of the C-terminal tag. Right panel: expression of doxycycline-regulated FLAG-SLC41A2-HA was analysed by immunoprecipitation with either anti-FLAG or anti-HA and then immunoblotting with the alternative antibody as indicated.

and similarity between our RT-PCR sequence and CAG32667/XP_425486, along with their homology with human SLC41A2 proteins, identifies these transcripts as encoding the chicken SLC41A2 homologue.

In order to functionally characterize human SLC41A2, we cloned a hSLC41A2 coding sequence in-frame with a FLAG tag under the control of a doxycycline-inducible promoter, and transfected this construct into HEK-293 cells (Figure 1C, left-hand panel). We observed doxycycline-induced expression of a band near the predicted 56 kDa molecular mass, consistent with the production of a full-length protein, along with a set of smaller bands in the 25–27 kDa range. We explored the origin of the faster-running bands by generating an *SLC41A2* expression construct tagged on the N-terminus with a FLAG epitope, and the C-terminus with an HA epitope, and analysing its behaviour by SDS/PAGE/Western blotting, followed by sequential anti-FLAG and anti-HA immunodetection (Figure 1C, middle panel). These experiments showed that two approx. 56 kDa bands, and at least two 25–27 kDa bands, are immunoreactive to both anti-FLAG and anti-HA. While the 56 kDa bands are likely to represent full-length protein, the lower-molecular-mass proteins could still represent partial degradation products, as these bands are approximately one-half the size of full-length protein. To evaluate this possibility, we immunoprecipitated with antibodies to each tag, followed by immunoblotting with the alternative tag (Figure 1C, right-hand panel), reasoning that degradation products would not be carried over in the immunoprecipitation, as co-precipitation experiments showed no evidence of SLC41A2 multimerization (results not shown). This experiment demonstrated that bands in both the 56 and 25–27 kDa ranges possess reactivity to both antibodies, suggesting that full-length protein can run at either a high or a low molecular mass. We speculate that the lower-molecular-mass bands represent anomalous migration of full-length protein due to its high hydrophobic residue content, as has been described for other hydrophobic proteins [14], whereas the higher-molecular-mass band represents unfolded SLC41A2, which disappears upon boiling due to heat-induced aggregation (see Supplementary Figure 2 at http://www.BiochemJ.org/bj/401/bj4010505add.htm, and [15–17]).

SLC41A2 is an N-terminus outside plasma-membrane protein

Although the above analyses indicated that our expression construct drives expression of a protein of the predicted size, the multiple sized products gave cause for concern as to whether properly folded and functional proteins were being expressed. Hydrophobicity analysis suggests an eleven-TM-span model of SLC41A2, consisting of two five-TM-span MgtE domains with the termini lying on opposite sides of whatever membranous compartment it resides in (Figure 2A). As a trans-plasma-membrane Mg^{2+} transport function would require at least some fraction of SLC41A2 to reside on the surface of the cell, and improperly folded proteins

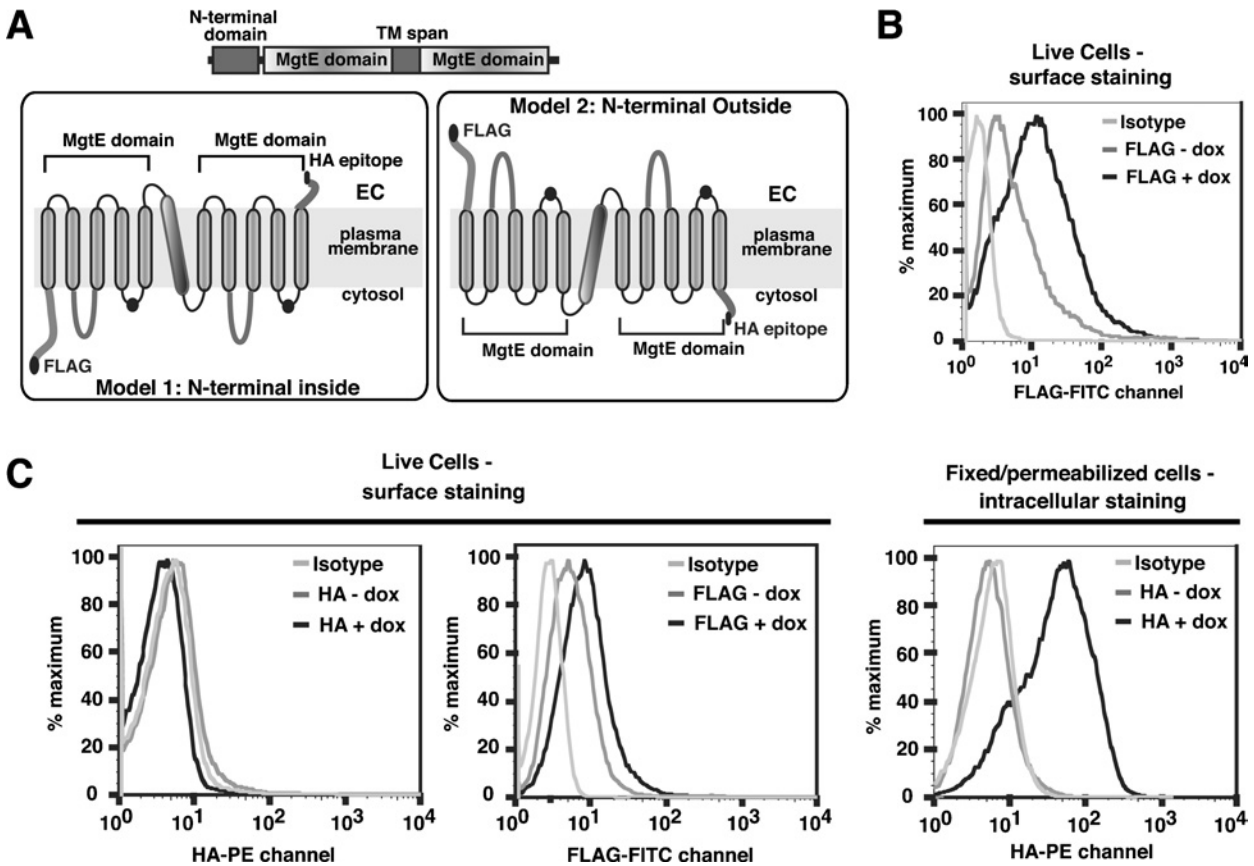

Figure 2 Surface expression and topological analysis of SLC41A2

(**A**) Domain structure of SLC41 proteins and most likely topological models based on the predicted five-TM structure for prokaryotic MgtE domains and the presence of an extra TM span between the MgtE domains of SLC41A2. (**B**) Anti-FLAG surface staining and flow cytometric analysis of FLAG–SLC41A2, demonstrating the presence of the N-terminal FLAG epitope on the extracellular side of the plasma membrane. (**C**) Anti-FLAG and anti-HA surface staining and flow-cytometric analysis of FLAG-SLC41A2-HA. For live cells, no signal is detected in the WT, uninduced or induced TRPM7 KO DT40 B-cells expressing FLAG-SLC41A2-HA (FLAG-tagged at the N-terminus and HA-tagged at the C-terminus) with PE/HA surface staining. However, after induction with doxycycline (dox; 1 μg/ml), FLAG-SLSC41A2-HA-expressing cells showed an increased fluorescence in comparison with both the isotype control (mouse IgG1-UNLB; Southern Biotech, Birmingham, AL, U.S.A.) and the uninduced cells after surface staining with FITC–FLAG, although to a lesser extent than the single-epitope-tagged FLAG-SLC41A2 cells. That the HA tag is accessible intracellularly is demonstrated by a dramatic shift in fluorescence in fixed/permeabilized PE-stained doxycycline-induced cells as compared with the isotype control and uninduced cells.

are generally prevented from being transported to the cell surface [18,19], we reasoned that either the N- or C-terminal tail of SLC41A2 should be detectable on the cell surface if our construct was driving expression of a well-folded functional protein. We initially tested this hypothesis by analysing SLC41A2 surface expression in a TRPM7-KO DT40 cell line inducibly expressing SLC41A2 with an N-terminal FLAG epitope (Figure 2B). As can be seen, anti-FLAG staining demonstrated abundant expression of anti-FLAG immunoreactivity on the cell surface after doxycycline induction, but very low levels in the absence of doxycycline, suggesting that our construct is able to drive expression of a properly folded and surface-expressed protein with an N-terminus-outside topology. We further evaluated the functionality and topology of SLC41A2 by performing anti-FLAG and anti-HA immunostaining of TRPM7-KO DT40 cells expressing double-tagged FLAG-SLC41A2-HA. Using surface staining with epitope tag-specific antibodies followed by flow cytometry (Figure 2C, left-hand panel), we observed a clear shift in fluorescence in FLAG staining after doxycycline induction as compared with the uninduced and isotype controls. The shift was smaller in magnitude than that observed for FLAG-SLC41A2, suggesting that FLAG-SLC41A2-HA does not surface transport as well as FLAG-SLC41A2. No change in fluorescence was observed upon doxycycline induction when α-HA antibody is used for surface labelling, indicating that the C-terminus of SLC41A2 is not accessible to extracellular staining antibodies. To confirm that the C-terminal HA tag is capable of binding to the anti-HA antibody reagent if it were accessible, FLAG-SLC41A2-HA expressing cells were fixed, permeabilized and stained with anti-HA antibody. In contrast with the anti-HA-stained live cells, where no shift in fluorescence is observed upon doxycycline induction, a large change in fluorescence is seen upon doxycycline induction for anti-HA-stained, fixed and permeabilized cells, confirming that the C-terminus is accessible intracellularly and capable of binding to the anti-HA antibody (Figure 2C, right-hand panel). An important point with regards to the interpretation of the results of these experiments is that there is ample precedent for N-terminal epitope tags not adversely influencing the membrane localization or topology of N-terminus-outside polytopic membrane proteins, the most notable examples being seven-TM-spanning G-protein-coupled receptors, nearly all of which tolerate N-terminal epitope tagging without significant alteration of surface expression or function [20,21].

Overall, the above results strongly support a plasma-membrane localization of SLC41A2 proteins with an odd-TM-span topology, as the N-terminal epitope tag is abundantly accessible to binding by extracellular antibody and the C-terminal tag is inaccessible. Although admittedly our data cannot discriminate

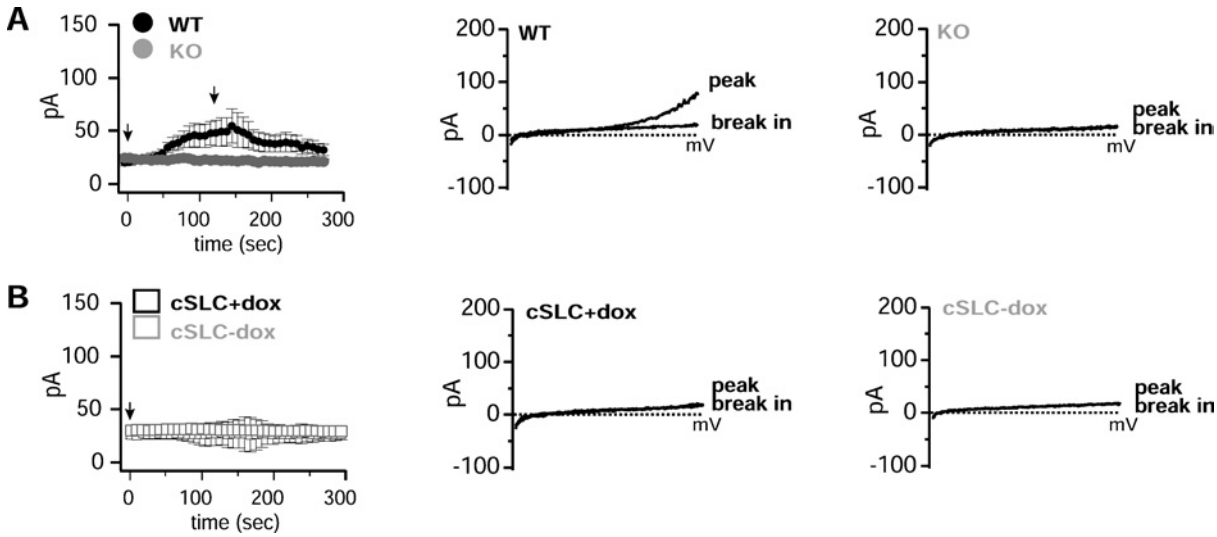

Figure 3 Patch-clamp analysis of WT, TRPM7-KO and SLC41A2-expressing TRPM7-KO cells

(**A**) Comparison of whole-cell currents evoked by dialysis with a nominally-zero-Mg^{2+}-containing intracellular solutions in WT and TRPM7-deficient DT40 cells. Left-hand panel: low-resolution graphs of current development over time. Middle panel: I/V curves at peak and break-in for WT DT40 cells, derived from a voltage ramp spanning −100 to +100 mv. Right-hand panel: I/V curves at peak (approx. 150 s) and break-in (beginning of recording) for TRPM7-deficient DT40 cells, derived in the same manner as for the middle panel. (**B**) Comparison of whole-cell currents evoked by dialysis with nominally-zero-Mg^{2+}-containing intracellular solutions in TRPM7-deficient DT40 cells before (− dox) and after (+ dox) induction of SLC41A2 expression with doxycycline. Left-hand panel: low-resolution graphs of current development over time. Middle panel: I/V curves at peak and break-in for induced cells, derived as in (**A**). Right-hand panel: I/V curves at peak and break-in for uninduced cells, derived as in (**A**). See the Experimental section for details of the electrophysiological protocols. pA in the ordinates indicates current in picoamperes.

among odd-TM-span models with different numbers of TM spans, in conjunction with the strong prediction of five TM spans in MgtE domains, and the presence of a TM span precisely between the two MgtE domains in SLC41A2, Occam's razor strongly favours an 11-TM-span model.

Analysis of membrane currents in SLC41A2-expressing DT40 cells

Expression of SLC41 proteins and MagT1 in oocytes has been reported to produce large membrane currents carried by Mg^{2+}, observations which have been used to impute an ion-channel Mg^{2+}-transport function to SLC41A1, SLC41A2, and MagT1 [4,5,7]. In order to evaluate the electrophysiological behaviour of SLC41A2 in detail, we analysed whole-cell currents by patch clamp in WT DT40, TRPM7-deficient DT40 cells, and TRPM7-deficient DT40 cells inducibly expressing or not SLC41A2 (Figure 3). In WT DT40 cells we observed the development of typical MIC (Mg^{2+}-inhibited cation current)/MagNUM (Mg^{2+}-nucleotide-regulated metal-ion current) currents, which activate under conditions of nominally zero intracellular Mg^{2+} and Mg-ATP, and physiological extracellular solutions (Figure 3A). These currents are completely absent in TRPM7-deficient DT40 cells, unequivocally identifying TRPM7 as the molecular substrate of MIC/MagNUM currents. Surprisingly, despite the demonstrated surface expression of SLC41A2 protein, no significant currents are observed under these conditions after SLC41A2 expression – SLC41A2-expressing TRPM7-deficient DT40 cells were indistinguishable from the same cells before induction or untransfected TRPM7-deficient DT40 cells (Figure 3B).

A lack of currents could be explained if our patch-clamp conditions resulted in SLC41A2 inactivation; however, we observed no differences in voltage ramps obtained even within 5–10 s of break between SLC41A2-expressing and non-expressing cells, suggesting to us that inactivation of SLC41A2 channels which were open prior to break in was probably not occurring. Another possibility is that the actual amount of current carried by Mg^{2+} was too small to resolve using physiological conditions. One approach to resolving small currents carried by bivalent-cation-selective ion channels is to remove all bivalent cations on one or both sides of the pool. This allows larger current flows carried by univalent ions (see, for example, [22, 23] for univalent flow through TRPM7). We performed such experiments comparing WT DT40 cells, TRPM7-deficient DT40 cells and TRPM7-deficient DT40 cells expressing SLC41A2 (Figure 4). In Figure 4(A), we utilized intracellular pipette conditions which included 5 mM EDTA to clamp intracellular Mg^{2+} to a very low level, and nominally bivalent-ion-free extracellular solution (e.g. no added Ca^{2+} or Mg^{2+}, but no added chelators). In Figure 4(B) we utilized solutions in which 5 mM EDTA was present in both intracellular and extracellular solutions. Although the altered solution conditions caused the expected and previously reported alterations in the TRPM7 I/V relationship [22,23], they did not resolve any novel currents in SLC41A2-expressing cells.

Overall, on the basis of the differences between our results and those of Goytain and Quamme [4], it appears that SLC41 family proteins may exhibit very different properties depending on the context in which they are expressed, a point which will be important to take into account in future investigations of SLC41 protein function.

Analysis of Mg^{2+} transport and growth after heterologous expression of SLC41A2 in TRPM7-deficient cells

On the basis of their expression on the DT40 cell surface, SLC41A2 proteins would be predicted to possess trans-plasma-membrane Mg^{2+} transport function. However, our inability to detect any apparent current flow associated with their expression suggested that they either are not functioning in trans-plasma-membrane Mg^{2+} transport or that their Mg^{2+} transport in the DT40 cell context is associated with current flows too small to easily detect using patch clamp. Such a situation might be expected, as net Mg^{2+} fluxes required to support cell division are very small,

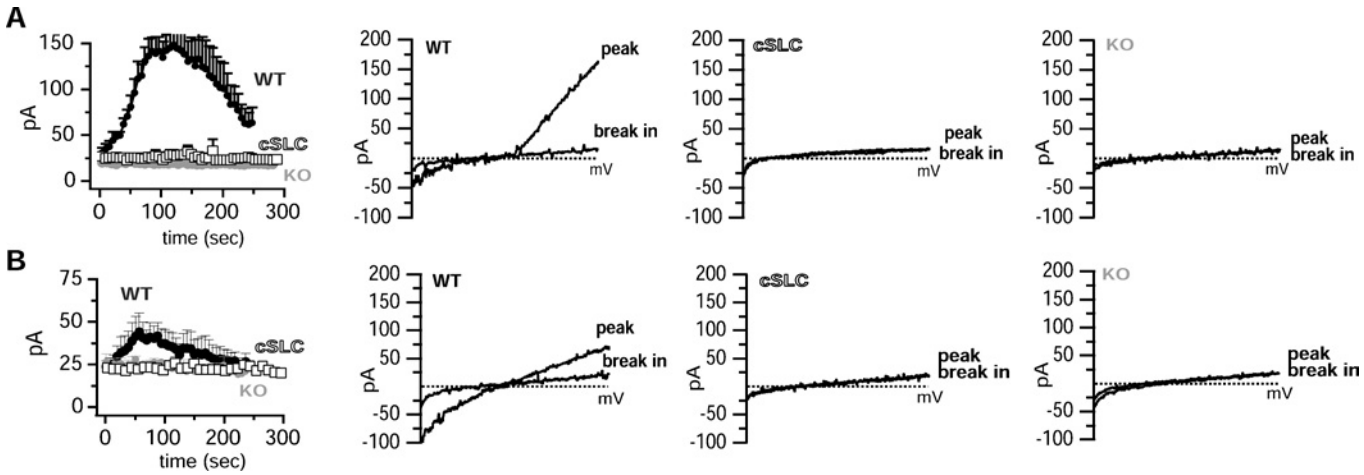

Figure 4 Patch-clamp analysis of WT, TRPM7-KO and SLC41A2-expressing TRPM7-KO cells under bivalent-ion-free conditions

(**A**) Comparison of whole-cell currents evoked by dialysis with a 5-mM-EDTA-containing intracellular solution and a nominally bivalent-ion-free extracellular solution. Note the enhanced outward currents associated with strong chelation of internal Mg^{2+}. Left panel: low-resolution graphs of current development over time. Second panel: I/V curves at peak (approx. 150 s) and break-in (beginning of recording) for WT DT40 cells. Third panel: I/V curves at peak and break-in for TRPM7-deficient DT40 cells expressing SLC41A2. Far-right (fourth) panel: I/V curves at peak and break-in for TRPM7-deficient DT40 cells. (**B**) Comparison of whole-cell currents evoked by dialysis with a 5-mM-EDTA-containing intracellular solution and a 5-mM-EDTA-containing extracellular solution. Note linearization of TRPM7 currents associated with strong chelation of bivalent cations on both sides of the TRPM7 pore. These changes are attributable to bidirectional univalent current flow through TRPM7 when the slower-permeating Mg^{2+} and Ca^{2+} ions are not present. Left-hand panel: low-resolution graphs of current development over time. Second panel: I/V curves at peak and break-in for WT DT40 cells. Third panel: I/V curves at peak and break-in for TRPM7-deficient DT40 cells expressing SLC41A2. Right-hand (fourth) panel: I/V curves at peak and break-in for TRPM7-deficient DT40 cells. All I/V curves are derived as described for Figure 3. See the Experimental section for details of electrophysiological protocols. pA in the ordinates indicates current in picoamperes.

or SLC41 protein could conceivably operate through a charge-neutral cation-exchange mechanism. In order to further evaluate their potential for trans-plasma-membrane Mg^{2+} transport, we analysed whether their expression altered net trans-plasma-membrane Mg^{2+} uptake or growth of TRPM7-deficient cells (Figure 5). We first analysed $^{26}Mg^{2+}$ uptake in DT40 WT, TRPM7-KO and TRPM7-deficient DT40 cells expressing N-terminally FLAG epitope-tagged SLC41A2 in the presence and absence of doxycycline from 0–8 h (Figure 5A, left panel). Mg^{2+} uptake as measured by the ratio of $^{26}Mg^{2+}/^{24}Mg^{2+}$ was approx. 2–3-fold higher in doxycycline-induced FLAG-SLC41A2-expressing cells as compared with the uninduced cells, and even greater than that observed in the WT DT40 cells, providing direct evidence that SLC41A2 overexpression correlates with enhanced Mg^{2+} accumulation. As expected, compared with the WT DT40 cells, very little Mg^{2+} transport occurs through endogenous Mg^{2+} uptake pathways in TRPM7-KO and uninduced cells.

As TRPM7-deficient cells have a proliferative defect which can be complemented by supplemental extracellular Mg^{2+}, enhanced Mg^{2+} uptake capacity provided by SLC41A2 expression would be predicted to correlate with an enhanced capacity to proliferate. This prediction was confirmed by analysis of the growth rates of FLAG-SLC41A2- and FLAG-SLC41A2-HA-expressing TRPM7-deficient DT40 cells in comparison with WT and unmanipulated TRPM7-deficient DT40 cells (Figure 5A, middle and right-hand panels). Although TRPM7-deficient DT40 cells induced to express FLAG-SLC41A2 or FLAG-SLC41A2-HA proliferated more slowly than WT DT40 cells in physiological levels of Mg^{2+}, in contrast with the TRPM7-deficient cells, they were able to proliferate continuously. Furthermore, the higher surface expression of FLAG-SLC41A2 relative to FLAG-SLC41A2-HA (as demonstrated in Figure 2) correlated with a more rapid rate of growth in physiological levels of Mg^{2+}, even though the FLAG-SLC41A2-HA cell line was able to grow as well as WT cells when provided with supplemental Mg^{2+} in the growth medium. These results suggested that a higher level of SLC41A2 expression directly supported a higher rate of Mg^{2+} uptake and consequently a higher rate of proliferation. We further confirmed that SLC41A2 expression level correlates with proliferation rate by performing a dose–response analysis using the FLAG-SLC41A2 expressing clone (Figure 5B). As can be seen, this analysis shows that higher doxycycline doses correlate with higher protein expression levels, higher surface expression of FLAG-SLC41A2, and higher rates of proliferation. Overall, these results show that SLC41A2 expression enhances both the Mg^{2+} uptake capacity and proliferation rate of TRPM7-deficient cells in the absence of supplemental Mg^{2+}, and does so in a manner which directly correlates with their level of expression on the cell surface, strongly supporting the hypothesis that SLC41A2 proteins directly mediate trans-plasma-membrane Mg^{2+} transport.

DISCUSSION

We have explored the use of a TRPM7-deficient DT40 cell line as a model system for identification of vertebrate Mg^{2+} transporters. On the basis of their homology with bacterial MgtE proteins, we cloned and characterized chicken and human homologues of an SLC41 family protein, SLC41A2, which we found expressed in both chicken and human lymphocytes. We show that although heterologous expression of human SLC41A2 in TRPM7-deficient DT40 cells produces a surface-expressed protein, its expression does not correlate with any novel whole-cell currents detectable by patch-clamp analysis. However, SLC41A2 expression in TRPM7-deficient cells is associated with an enhanced rate of Mg^{2+} accumulation, endows them with proficiency for growth in medium without supplemental Mg^{2+} and enhances their rate of proliferation in proportion to SLC41A2 surface expression level. Overall, our results suggest that SLC41A2 functions within a vertebrate Mg^{2+}-uptake pathway as a trans-plasma-membrane Mg^{2+} transporter, and validate the use of TRPM7-KO cells as a system for identifying and studying molecular mechanisms involved in vertebrate Mg^{2+} homoeostasis.

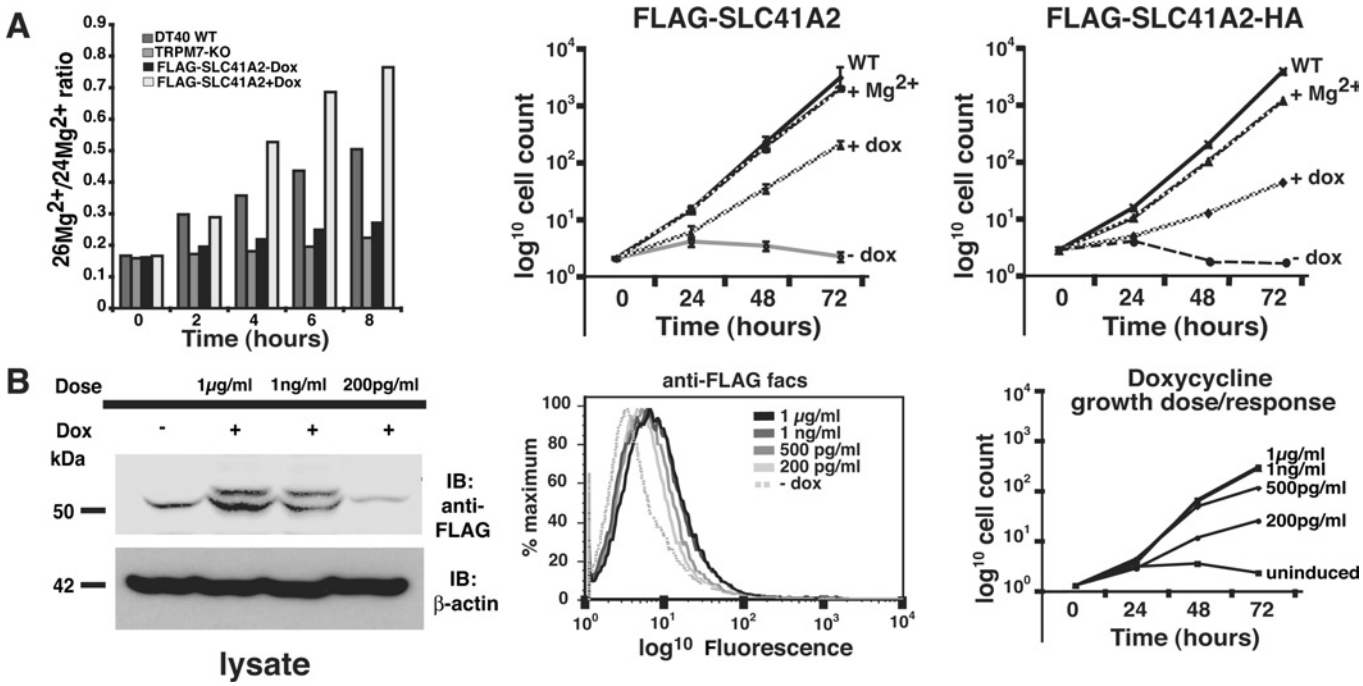

Figure 5 SLC41A2 expression correlates with enhanced Mg^{2+}-uptake and growth of TRPM7-KO cells

(**A**) Left-hand panel: DT40 WT, TRPM7-KO and TRPM7-KO cells complemented with SLC41A2 were grown in the presence (+dox) or absence (−dox) of doxycycline in cell-culture medium containing FBS, 0.4 mM $^{26}Mg^{2+}$and residual Mg^{2+} present in the FBS in the natural isotopic ratio. Cells were lysed at the indicated time intervals after addition of $^{26}Mg^{2+}$, and $^{26}Mg^{2+}/^{24}Mg^{2+}$ ratios were determined using mass spectrometry (ICP-MS). As a control, the $^{25}Mg^{2+}/^{24}Mg^{2+}$ ratio was determined for each sample and showed no variation, demonstrating the expected conserved natural abundance ratio in all samples (result not shown). Middle and right-hand panels: growth curves after induction of FLAG-SLC41A2 ($n = 6$) and FLAG-SLC41A2-HA expression respectively. Cells were cultured under defined conditions and their growth was plotted on an exponential scale. S.D. was calculated for FLAG-SLC41A2-expressing cells, as shown in the middle panel, and was determined to be 0 for all cell lines at the starting time point of 0. For certain time points the S.D. was smaller than the point symbol. WT and TRPM7-KO cells with Mg^{2+} are shown as controls. WT, wild-type; + Mg^{2+}, TRPM7-deficient cells with 15 mM supplemental Mg^{2+} added to the growth medium; − dox: no doxycycline added; + dox: 1 μg/ml doxycycline added. (**B**) Dose-dependence of SLC41A2-supported growth. FLAG-SLC41A2-expressing DT40 cells were induced with various concentrations of doxycycline and the level of overall expression (left-hand panel), surface expression (middle panel) and growth rates (right-hand panel) were analysed. Overall expression was analysed by SDS/PAGE and anti-FLAG immunoblotting, surface expression was analysed by anti-FLAG staining and FACS, and growth was analysed by cell counting as described in the Experimental section. Abbreviation: IB, immunoblotting.

Although our results are superficially consistent with other recent reports that SLC41A1 and SLC41A2 are Mg^{2+} transporters, these reports correlated SLC41A1 and SLC41A2 RNA injection with the appearance of large Mg^{2+}-selective currents in SLC41A1/A2 RNA-injected *Xenopus* oocytes [4,5]. Since we are not able to detect any apparent currents which correlate with SLC41A2 expression in TRPM7-deficient DT40 cells, despite their capacity to inducibly complement the defects in Mg^{2+} uptake and growth of these cells, it seems that SLC41A2 regulation or function in its native vertebrate cellular context differs significantly from that observed in the oocyte system. Resolving the differences between the behaviour of SLC41 proteins observed in our vertebrate system versus that observed in the oocyte expression system will be important for generating a clearer understanding of the Mg^{2+}-transport mechanism and regulation of SLC41 proteins.

Our results also provide important information for future structure–function analyses of SLC41 family proteins, in the form of evidence that supports an 11-TM-span model for the SLC41 family. Two important predictions of an 11-TM-span model for SLC41 family proteins stand out. First, such a model places the two MgtE domains in the same orientation, suggesting that either they dimerize to form a functional transporter/channel, or that each SLC41 family member has two discrete channel/transporter domains. Secondly, on the basis of the extracellular position of a conserved negative charge motif found in each MgtE domain (black dot in MgtE domains of Figure 2), and the trans-plasma-membrane Mg^{2+}-transport function supported by the data in this manuscript, an 11-TM-span model places this motif at the entrance side of the transporter/channel. This would support the hypothesis that this motif might represent a form of Mg^{2+}-binding site or selectivity filter.

Our results raise important questions regarding the relative roles of TRPM7 and SLC41A2 family proteins in Mg^{2+} uptake and homoeostasis in vertebrate cells. Whereas deficiency of TRPM6 or TRPM7 function are clearly associated with markedly decreased Mg^{2+} accumulation [1–3], the existence of a second physiologically relevant Mg^{2+}-uptake mechanism mediated by SLC41 proteins suggests the need to re-examine TRPM6/TRPM7′s direct role(s) in Mg^{2+} uptake and their overall contribution to Mg^{2+} uptake under different conditions. Furthermore, the observation that DT40 cells normally express both TRPM7 and SLC41A2 suggests that the forces driving the creation of the complex TRPM7 channel/kinase fusion protein must involve processes more complex than the requirement for a Mg^{2+} permeation/uptake mechanism, as the MgtE scaffold would have been readily available for that purpose from the earliest branch points in evolution of multicellular organisms. One encompassing explanation for the existence of both TRPM6/7 and SLC41 proteins would be that TRPM6/7 have dominant roles in Mg^{2+} uptake in physiological situations where receptor-regulated Mg^{2+} uptake is required, such as Mg^{2+} uptake required for organismal Mg^{2+} homoeostasis, cell growth or neuronal function. SLC41 proteins might then primarily provide a background level of Mg^{2+} uptake required to maintain Mg^{2+} homoeostasis under ‘static’ conditions.

This scenario is supported by the apparent ubiquitous high-level expression of SLC41A2 transcripts observed in large-scale analyses of mouse and human transcriptomes [e.g. GDS592 and GDS593 records in Entrez GEO (http://www.ncbi.nlm.nih.gov/geo/) profiles]. This scenario would also explain the dominant role that TRPM7 appears to have in Mg^{2+} uptake into rapidly proliferating immune cells, as well as its prominent expression in kidney and metabolically active cells such as neurons. Alternatively, TRPM7 may act primarily as a Mg^{2+} sensor through its dual channel/kinase functions and, secondarily, regulate a quantitatively more important direct Mg^{2+} uptake pathway mediated through the function of SLC41 proteins or participate in a similar fashion in some other as yet unidentified Mg^{2+} regulatory mechanisms. Dissecting the relative contributions of SLC41 proteins and TRPM6/7 to Mg^{2+} uptake and regulation of Mg^{2+} homoeostasis occurring in different tissues and under various conditions are important goals for future investigations.

We thank Dr Almut Meyer-Bahlburg, Ms Sarah Andrews, Mr Ashok Bandaranayake, Mr Alexander Astrakhan and Mr Noel Blake (University of Washington and Children's Hospital and Regional Medical Center, Seattle, WA, U.S.A.) for their help and their insightful and valuable suggestions. This work was supported by National Institutes of Health (NIH) grant GM64316.

REFERENCES

1 Schlingmann, K. P., Weber, S., Peters, M., Niemann Nejsum, L., Vitzthum, H., Klingel, K., Kratz, M., Haddad, E., Ristoff, E., Dinour, D. et al. (2002) Hypomagnesemia with secondary hypocalcemia is caused by mutations in TRPM6, a new member of the TRPM gene family. Nat. Genet. **31**, 166–170

2 Schmitz, C., Perraud, A. L., Johnson, C. O., Inabe, K., Smith, M. K., Penner, R., Kurosaki, T., Fleig, A. and Scharenberg, A. M. (2003) Regulation of vertebrate cellular Mg^{2+} homeostasis by TRPM7. Cell **114**, 191–200

3 Walder, R. Y., Landau, D., Meyer, P., Shalev, H., Tsolia, M., Borochowitz, Z., Boettger, M. B., Beck, G. E., Englehardt, R. K., Carmi, R. and Sheffield, V. C. (2002) Mutation of TRPM6 causes familial hypomagnesemia with secondary hypocalcemia. Nat. Genet. **31**, 171–174

4 Goytain, A. and Quamme, G. A. (2005) Functional characterization of the human solute carrier, SLC41A2. Biochem. Biophys. Res. Commun. **330**, 701–705

5 Goytain, A. and Quamme, G. A. (2005) Functional Characterization of human SLC41A1, a Mg^{2+} transporter with similarity to prokaryotic MgtE Mg^{2+} transporters. Physiol. Genom. **22**, 382–389

6 Wabakken, T., Rian, E., Kveine, M. and Aasheim, H. C. (2003) The human solute carrier SLC41A1 belongs to a novel eukaryotic subfamily with homology to prokaryotic MgtE Mg^{2+} transporters. Biochem. Biophys. Res. Commun. **306**, 718–724

7 Goytain, A. and Quamme, G. A. (2005) Identification and characterization of a novel mammalian Mg^{2+} transporter with channel-like properties. BMC Genom. **6**, 48

8 Coudray, C., Pepin, D., Tressol, J. C., Bellanger, J. and Rayssiguier, Y. (1997) Study of magnesium bioavailability using stable isotopes and the inductively-coupled plasma mass spectrometry technique in the rat: single and double labelling approaches. Br. J. Nutr. **77**, 957–970

9 Stegmann, W. and Quamme, G. A. (2000) Determination of epithelial magnesium transport with stable isotopes. J. Pharmacol. Toxicol. Methods **43**, 177–182

10 Merino, S., Gavin, R., Altarriba, M., Izquierdo, L., Maguire, M. E. and Tomas, J. M. (2001) The MgtE Mg^{2+} transport protein is involved in *Aeromonas hydrophila* adherence. FEMS Microbiol. Lett. **198**, 189–195

11 Smith, R. L. and Maguire, M. E. (1998) Microbial magnesium transport: unusual transporters searching for identity. Mol. Microbiol. **28**, 217–226

12 Smith, R. L., Thompson, L. J. and Maguire, M. E. (1995) Cloning and characterization of MgtE, a putative new class of Mg^{2+} transporter from *Bacillus firmus* OF4. J. Bacteriol. **177**, 1233–1238

13 Townsend, D. E., Esenwine, A. J., George, 3rd, J., Bross, D., Maguire, M. E. and Smith, R. L. (1995) Cloning of the mgtE Mg^{2+} transporter from *Providencia stuartii* and the distribution of mgtE in Gram-negative and Gram-positive bacteria. J. Bacteriol. **177**, 5350–5354

14 Luthi, E., Baur, H., Gamper, M., Brunner, F., Villeval, D., Mercenier, A. and Haas, D. (1990) The arc operon for anaerobic arginine catabolism in *Pseudomonas aeruginosa* contains an additional gene, *arcD*, encoding a membrane protein. Gene **87**, 37–43

15 Blakey, D., Leech, A., Thomas, G. H., Coutts, G., Findlay, K. and Merrick, M. (2002) Purification of the *Escherichia coli* ammonium transporter AmtB reveals a trimeric stoichiometry. Biochem. J. **364**, 527–535

16 Borgnia, M. J., Kozono, D., Calamita, G., Maloney, P. C. and Agre, P. (1999) Functional reconstitution and characterization of AqpZ, the*EE. coli* water channel protein. J. Mol. Biol. **291**, 1169–1179

17 Hyman, M. R. and Arp, D. J. (1993) An electrophoretic study of the thermal- and reductant-dependent aggregation of the 27 kDa component of ammonia monooxygenase from *Nitrosomonas europaea*. Electrophoresis **14**, 619–627

18 Arvan, P., Zhao, X., Ramos-Castaneda, J. and Chang, A. (2002) Secretory pathway quality control operating in Golgi, plasmalemmal, and endosomal systems. Traffic **3**, 771–780

19 Ma, Y. and Hendershot, L. M. (2001) The unfolding tale of the unfolded protein response. Cell **107**, 827–830

20 Amstrup, J. and Novak, I. (2003) P2X7 receptor activates extracellular signal-regulated kinases ERK1 and ERK2 independently of Ca^{2+} influx. Biochem. J. **374**, 51–61

21 Ivic, L., Zhang, C., Zhang, X., Yoon, S. O. and Firestein, S. (2002) Intracellular trafficking of a tagged and functional mammalian olfactory receptor. J. Neurobiol. **50**, 56–68

22 Nadler, M. J., Hermosura, M. C., Inabe, K., Perraud, A. L., Zhu, Q., Stokes, A. J., Kurosaki, T., Kinet, J. P., Penner, R., Scharenberg, A. M. and Fleig, A. (2001) LTRPC7 is a Mg·ATP-regulated divalent cation channel required for cell viability. Nature **411**, 590–595

23 Prakriya, M. and Lewis, R. S. (2002) Separation and characterization of currents through store-operated CRAC channels and Mg^{2+}-inhibited cation (MIC) channels. J. Gen. Physiol. **119**, 487–507

Received 5 May 2006/5 September 2006; accepted 19 September 2006
Published as BJ Immediate Publication 19 September 2006, doi:10.1042/BJ20060673